Biophysical Journal
Article

Single-Molecule Assay for Proteolytic Susceptibility: Force-Induced Collagen Destabilization

Michael W. H. Kirkness[1] and Nancy R. Forde[1,2,*]
[1]Department of Molecular Biology and Biochemistry and [2]Department of Physics, Simon Fraser University, Burnaby, British Columbia, Canada

ABSTRACT Force plays a key role in regulating dynamics of biomolecular structure and interactions, yet techniques are lacking to manipulate and continuously read out this response with high throughput. We present an enzymatic assay for force-dependent accessibility of structure that makes use of a wireless mini-radio centrifuge force microscope to provide a real-time readout of kinetics. The microscope is designed for ease of use, fits in a standard centrifuge bucket, and offers high-throughput, video-rate readout of individual proteolytic cleavage events. Proteolysis measurements on thousands of tethered collagen molecules show a load-enhanced trypsin sensitivity, indicating destabilization of the triple helix.

INTRODUCTION

The conventional view of fixed protein structure is evolving toward one of dynamic conformational sampling. This change in perspective requires techniques to interrogate structures that are not static. Although the structural technique of NMR spectroscopy offers atomic-level resolution of time-averaged dynamics of small proteins in solution, it lacks the ability to resolve larger structures and complexes. For larger systems, transient accessibility of otherwise buried regions can be identified and quantified using enzymatic cleavage assays (1–3). These assays provide significant insight into structural stability, but because they require electrophoretic analysis of products extracted at discrete time points, the assays lack real-time monitoring of reaction progress. Furthermore, none of these assays assesses the modification of structures by applied force. Force is an increasingly apparent regulator of cellular activity, wherein mechanical actuation of cryptic sites in proteins can control downstream signaling (4). There is a need for new methods capable of reading out, in real time, changes in protein conformation resulting from external stimuli such as applied force.

Here, we introduce the technique of high-throughput, force-dependent proteolysis using a mini-radio centrifuge force microscope (MR.CFM), which enables the real-time assessment of molecular structural stability. As proof of concept, we assess the force-dependent modulation of collagen's triple helical structure.

Collagen is a key component of the extracellular matrix and is the predominant protein in vertebrates, where it confers tensile strength to connective tissues (5,6). Collagen is a hierarchically structured material: individual triple-helical collagen proteins assemble into highly ordered fibrils, which in turn are the building blocks for fibers, a wide range of connective tissues, and the extracellular matrix. How these are regulated by applied load, in particular their susceptibility to enzymatic remodeling, has direct relevance to their physiological performance. Numerous studies have reached contradictory conclusions about how applied force influences the proteolytic susceptibility of collagen at different hierarchical scales, and a clear mechanistic interpretation of the varied results remains elusive (6,7). Understanding how collagen is affected by stress is complicated by the embedded hierarchical structural levels and their respective responses to force.

At the molecular level, collagen is distinguished by its unique triple-helical structure. This structure prevents conventional proteolysis and requires specialized collagenases for its degradation (8). Not surprisingly, given its mechanical importance, there has been substantial interest in understanding how the triple helix deforms when stretched. However, previous studies have reached contradictory conclusions about how the triple helix is modified

Submitted August 16, 2017, and accepted for publication December 11, 2017.

*Correspondence: nforde@sfu.ca

Editor: Alexander Dunn.
https://doi.org/10.1016/j.bpj.2017.12.006

© 2017 Biophysical Society.

by applied force (Table 1): does it entropically extend, shear open, unwind, or tighten? These investigations each have limitations: model peptide sequences lack the context of the full-length protein (6,9); triple-helical stability can depend on the force field used in simulations (6,10,11); changes in length of the full protein observed under force do not reveal structural or sequence-dependent information (12,13); and collagenases used to investigate force-induced deformations (9,14,15) are not inert probes, because their specialized proteolysis of intact collagen derives from their ability to manipulate its triple-helical structure (8,16).

To resolve the question of how collagen's structure is altered by force, we implement the hallmark assay for triple-helical stability, trypsin susceptibility (1), enhancing its utility by incorporating force into single-molecule proteolysis assays. A tight triple helix blocks proteolytic cleavage by presenting a steric barrier that prevents access of a single polypeptide chain to trypsin's active site. Thus, only if collagen's structure locally denatures can cleavage by trypsin occur (1). If a stretching force destabilizes the triple helix, an increase in the proteolysis rate should be observed (Fig. 1). Conversely, if no change in structure occurs, or if the helix tightens, the cleavage rate should remain unchanged or be reduced. To assess the effect of force on collagen's stability, we use MR.CFM to probe thousands of individual collagen molecules and determine how force affects their rate of proteolysis by trypsin.

MATERIALS AND METHODS

MR.CFM

MR.CFM is a wireless, fully self-contained, compact bright-field microscope (Fig. 2) that exploits the rotation of a commercial benchtop centrifuge to exert controlled force. MR.CFM fits within a single bucket of a Beckman Coulter (Brea, CA) Allegra X-12R centrifuge, equipped with an SX4750A ARIES Swinging Bucket Rotor assembly. This assembly has an imbalance tolerance of ±50 g. MR.CFM was built using as many commercial parts as possible for ease of reproduction. The final height and weight for MR.CFM are 154 mm and 421 g (including batteries), respectively. These fall well within the length and weight budgets of the centrifuge rotor.

TABLE 1 Reported Force-Dependent Responses of Collagen's Triple Helix for Forces below 10 pN

Force Response	Technique Used
Stabilizes/tightens	force-dependent cleavage with bacterial collagenase (14)
	steered molecular dynamics (6)
No change (entropically extends)	optical tweezers stretching (12)
	steered molecular dynamics (6)
	force-dependent cleavage with bacterial collagenase (15)
Destabilizes/unwinds/lengthens	force-dependent cleavage with MMP1 (9,15)
	optical tweezers stretching (13)
Shears open	steered molecular dynamics (10)

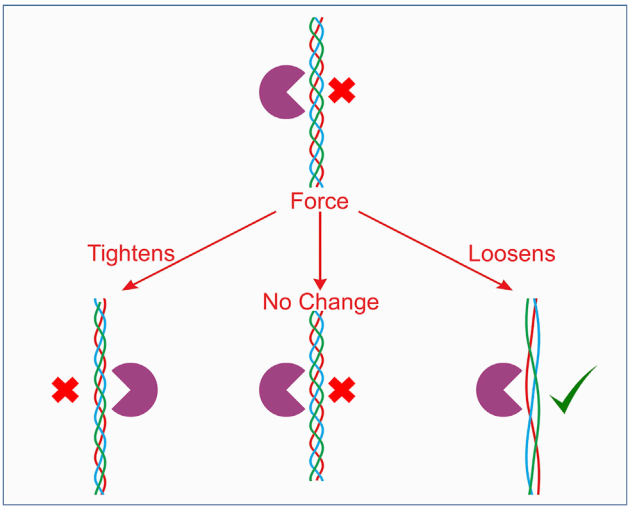

FIGURE 1 Possible responses of collagen's triple helix to applied stress. In the absence of applied force, a stable triple helix is resistant to proteolysis by trypsin (*upper*). If the helix tightens or remains unchanged by force (*lower left* and *center*, respectively), it remains resistant to cleavage by trypsin. Only if force induces a destabilization of the helix will proteolysis by trypsin be possible (*lower right*). To see this figure in color, go online.

Schematics and parts lists are provided in Fig. S1 and Table S1, with a description of the design provided in the Supporting Materials and Methods. Drawings of the few custom parts are provided in Fig. S2 and in computer-aided drawings in Data S1. Note that although the designs provided are specific to this rotor assembly, MR.CFM can easily be adapted for other benchtop centrifuges, primarily by modifying the base.

Image acquisition and particle detection

The image-analysis workflow to acquire, process, and analyze data from the raw image stream is shown schematically in Fig. 3 and is described in the Supporting Materials and Methods. The ImageJ macro written for image processing is provided as Data S2. Particles are counted with the Mosaic particle tracker 2D/3D plugin for ImageJ (17).

MR.CFM sample chambers

Glass slides and coverslips were cut to 12 mm × 33 mm to fit the sample holder. Sample chambers were created between a coverslip (borosilicate glass no. 1; VWR, 48393 106) and a glass slide (soda lime glass 2 mm, Logitech Limited, Newark, CA) by strips of glue (JB Weld, Atlanta, GA), with a depth of ~300 μm.

Surface chemistry

We implemented a blocking and specific tethering system that relies on a self-assembled monolayer of Tween-20 for blocking and on biotinylated bovine serum albumin (BSA) for specific tethering. Modifications to the published protocol for surface blocking (18) are provided in the Supporting Materials and Methods.

Collagen functionalization

Type III collagen was used in these experiments due to its chemically accessible C-terminal cysteine residues, unique among fibrillar collagens. Recombinant human type III collagen (Fibrogen FG-5016) was end-labeled

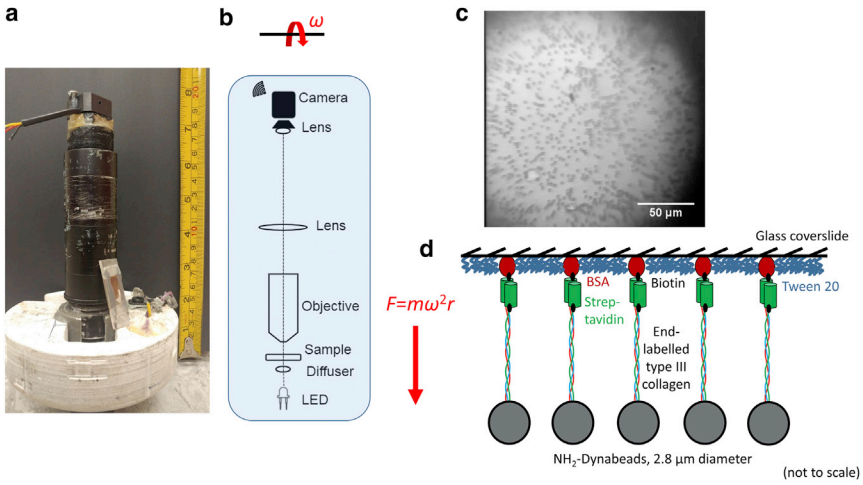

FIGURE 2 Mini-radio centrifuge force microscope (MR.CFM) and collagen tethering. (*a*) Photograph of the microscope, with the centrifuge bucket insert at the bottom and a sample chamber leaning at the side. The height of the assembly is <16 cm and its mass is 421 g. (*b*) Schematic of the optical elements within the microscope. A force $F = m\omega^2 r$ is exerted on all beads of relative mass m within the sample chamber, located a distance r from the central rotation axis, when the rotor spins at angular frequency ω. (*c*) Image of microspheres subjected to 9 pN of force in MR.CFM, tethered to the surface by collagen molecules. Although each bead occupies only a few pixels in the final image, they are easily detected. (*d*) Schematic of tethering geometry. Single molecules of collagen are tethered to a glass slide via biotin-streptavidin linkages, and are covalently linked to the surface of heavy beads via thiol-amine coupling. To see this figure in color, go online.

for manipulation as previously described (19), with information provided in the Supporting Materials and Methods. Briefly, this approach utilized biotinylation of introduced N-terminal aldehydes and covalent linking of C-terminal thiols to amine-functionalized superparamagnetic microspheres (2.8 μm diameter, M270 Dynabeads).

Single-molecule proteolysis experiments

All trypsin cleavage experiments were performed at room temperature with the following final concentrations: trypsin (T1426; Sigma Aldrich, St. Louis, MO) 2.0 mg/mL, 1× reaction buffer (0.1 M Tris and 0.4 M NaCl, pH 7.4), and collagenated beads ($<10^8$ beads/mL). To minimize room-temperature proteolysis of collagen by trypsin (Fig. S3), all solutions were kept at 4°C before use. Control experiments on DNA used aldehyde- and thiol-functionalized DNA (see Supporting Materials and Methods). Experiments at 9 pN of force were performed in MR.CFM, whereas zero-force (67 fN) experiments utilized a bright-field microscope (BX51; Olympus, Tokyo, Japan, equipped with 10× Plan N objective). Detailed experimental protocols are provided in the Supporting Materials and Methods, as is information about the number of distinct experimental runs for each condition.

The number of potential trypsin cleavage sites in type III collagen was given by the Expasy PeptideCutter tool (20), querying from sites 154 to 1221 of UniProtKB: P02461. This sequence represents the collagen domain of human type III procollagen.

Data analysis

Fitting of the decay data with Eq. 2 was performed in IGOR Pro (WaveMetrics, Lake Oswego, OR), weighted by the errors associated with each point. Data were analyzed following three separate approaches: determining from all replicates the mean fraction remaining as a function of time (where the error used was the standard error of the mean) (Fig. 4; Table 2); pooling all replicates to analyze the fraction of the total beads remaining as a function of time (where the error was taken to be a $\sqrt{N_{\mathrm{tot}}(t)}$ counting error) (Table S2 for collagen and Fig. S4 for DNA); and by fitting each individual replicate to Eq. 1 (where the error at each time point was taken to be a $\sqrt{N(t)}$ counting error) and determining the mean of these rates (Table S3 for collagen and Table S4 for DNA). Fit parameters are presented as best-fit values ± SD. To determine whether force enhances or hinders collagen proteolysis, we compared the trypsin-dependent rates $k_{\mathrm{Tr,F}}$ and $k_{\mathrm{Tr,0}}$.

RESULTS AND DISCUSSION

MR.CFM

To perform high-throughput proteolysis assays in a force-dependent manner, we developed an instrument dubbed the MR.CFM (Fig. 2). Centrifuge force microscopy requires

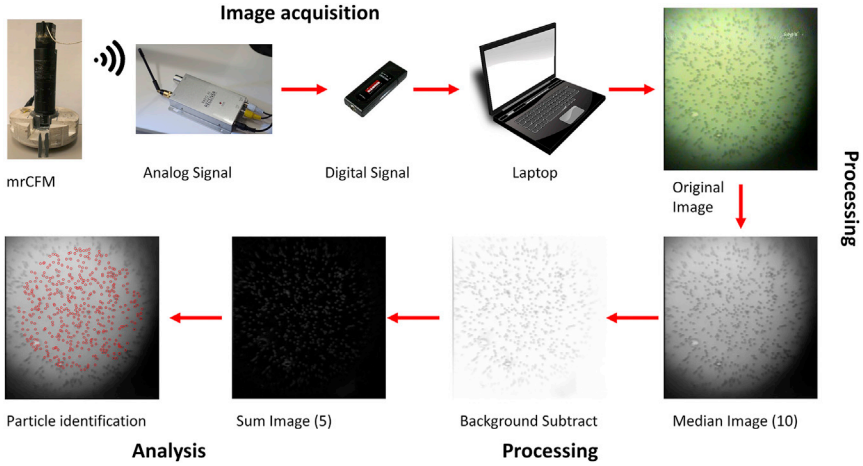

FIGURE 3 Work flow for MR.CFM acquisition, processing, and analysis of bead images. Images are acquired with the wireless camera in MR.CFM, then transmitted via radio signal to the audiovisual receiver. The audiovisual receiver collects the analog signal, which is output to a USB analog-to-digital converter attached to a laptop computer, where the image stream is simultaneously visualized in real time and stored. The original output image files from MR.CFM (shown here at 9 pN of force) are processed in ImageJ to improve contrast and remove rotation-speed-dependent interference. Particles are counted using the Mosaic particle-tracking program. The resultant overlaid image visually shows that this procedure is robust and identifies beads within the defined search area. To see this figure in color, go online.

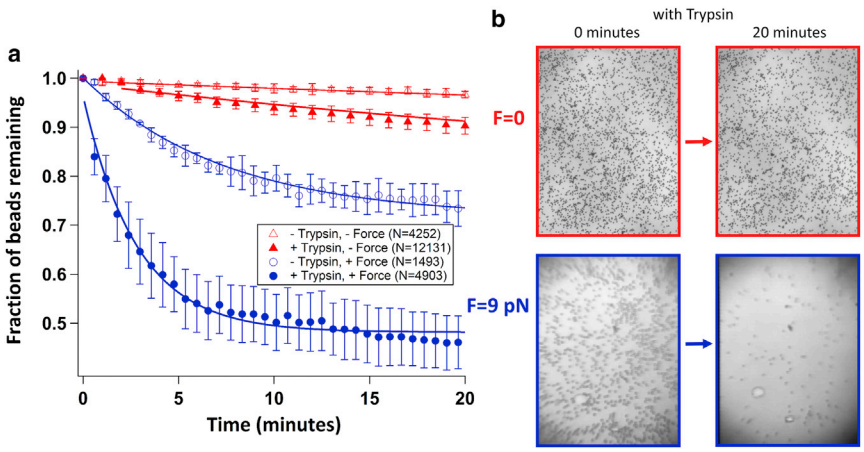

FIGURE 4 Collagen proteolysis by trypsin is enhanced by force. (*a*) Collagen tethers rupture at higher rates in the presence of force and trypsin (*solid blue circles*) than in the absence of either, implying their force-induced denaturation. Data points represent the mean fraction of beads remaining at each time and error bars represent standard errors of this mean. Every 10th data point is shown for the experiments at 9 pN of force, for clarity. Each experimental condition is well described by a single-exponential decay process, with rate constants presented in Table 2. (*b*) Representative images of collagen-tethered beads at the beginning (*left*) and after 20 min (*right*) of incubation with trypsin. Top: no force (67 fN; gravitational force on beads), recorded using a conventional bright-field microscope. Bottom: 8.8 pN of force, recorded within MR.CFM. To see this figure in color, go online.

only a microscope capable of stable imaging at high acceleration and dense particles on which to exert force, and can have a force range orders of magnitude larger than that of magnetic or optical tweezers (21). Our instrument was designed to be easily adopted by biological research labs, as it is a "plug-and-play," modular, entirely wireless bright-field microscope that can be placed into the bucket of a conventional benchtop centrifuge, counterbalanced simply by tubes of water. The force is determined by the rotational frequency of the centrifuge, ω (typically hundreds to thousands of rotations per minute), the distance between the sample and the axis of rotation, r (typically tens of centimeters), and the mass of the bead, m (relative to the displaced water), tethered to the molecule of interest: $F = m\omega^2 r$. Unlike the limited region of constant force in alternative single-molecule force techniques (22), the CFM provides a controllable, uniform force across the entire rotating sample chamber.

The layout of MR.CFM was driven by optical simplicity and low mass. Thus, in contrast to alternative approaches (23,24), our instrument has a straight optical path and requires no mirrors. Besides ease of optical design, the straight layout positions the camera closer to the center of rotation, subjecting it to less force during operation. In addition to substantially reduced cost, MR.CFM affords significant advantages over previous compact designs by 1) utilizing an unmodified centrifuge, thereby being amenable to use in shared facilities (24); and 2) offering continuous radio-frequency video output, permitting unlimited video-rate capture and digitization (23). The latter advantage confers the ability to read out molecular kinetics over experimental timescales of hours, without the need to sacrifice temporal resolution.

With a CFM, throughput is limited only by the ability to resolve individual tethered particles. In our instrument, image quality is limited by the camera, which was selected to provide exceptional value for financial and weight budgets: the image quality is sufficient for bead detection and the "binary" decision about the presence or absence of a bead (see below); the analog radio-frequency signal can be captured and digitized at video rates in real time; the cost of the camera is only $25 USD at the time of this writing; and the camera mass is only 9 g. Moreover, because each camera unit has a unique radio frequency output, further multiplexing of experiments would involve simply cloning MR.CFM with a different camera unit, and capturing video streams to the computer from parallel experiments within one centrifuge.

A wide field of view and high-efficiency surface chemistry enable the simultaneous visualization of hundreds of particles. High-throughput analysis is enabled by manipulating the raw image stream acquired by MR.CFM and computationally detecting and counting scores of particles (Fig. 3). The image processing used in this work minimizes user input and is implemented within a semi-automated ImageJ macro. With the use of this macro, beads occupying only a few pixels in the wide-field images from MR.CFM can be easily detected.

TABLE 2 Rate Constants Obtained for Collagen Bead Detachment

Experiment	k_{eff} (min^{-1})	k_{ns} (min^{-1})	k_{Tr} (min^{-1})
− trypsin, $F = 0$	–	0.010[a] ± 0.013	–
+ trypsin, $F = 0$	0.020 ± 0.001	0.010[b] ± 0.013	0.009 ± 0.013
− trypsin, $F = 9$ pN	–	0.135 ± 0.003	–
+ trypsin, $F = 9$ pN	0.357 ± 0.018	0.135[b] ± 0.003	0.222 ± 0.018

Rate constants were determined by weighting $\langle f(t) \rangle$ by the mean ± SE.
[a]Determined by weighting $f(t)$ by counting error (Table S2), as the mean ± SE-based $k_{ns} = 0.007$ min^{-1} carried a very high uncertainty.
[b]Values from the no-enzyme fits were used to determine the trypsin-dependent rate constants, using Eqs. 1 and 2.

Collagen proteolysis under force

To determine whether tension affects stability of collagen's triple helix, we determined how an applied force alters its rate of cleavage by trypsin. Single type III collagen

molecules were tethered by a heavy microsphere to a surface, and force was applied from gravity ($F = 0.067$ pN ≈ 0) or by force from rotation of a centrifuge (Fig. 2 *d*). Tether-rupture kinetics were measured in the presence and absence of trypsin. Movie S1 provides an example experimental data set with collagen strained by 9 pN of force, in the presence of trypsin.

From measurements on thousands of distinct single-molecule tethers, our data show a significantly enhanced rate of collagen cleavage by trypsin in the presence of applied force (Figs. 4 and S5). For each experimental condition, the fraction of beads remaining as a function of time, $f(t)$, was well described by a single-exponential decay process. Thus, the data were fit to obtain first-order effective rate constants:

$$f(t) = A_{\text{eff}} e^{-k_{\text{eff}} t} + f_{\text{o}}. \tag{1}$$

Bead loss in the absence of trypsin was ascribed to nonspecific detachment, such that $k_{\text{eff}} = k_{\text{ns}}$. In the presence of trypsin, two competing processes contribute to bead loss, nonspecific detachment and trypsin-dependent cleavage; thus, $k_{\text{eff}} = k_{\text{ns}} + k_{\text{Tr}}$. Both k_{ns} and k_{Tr} depend on force, giving

$$f_{\text{ns},\,i}(t) = A_{\text{ns},\,i} e^{-k_{\text{ns},i} t} + f_o, \tag{2a}$$

$$f_{\text{Tr},\,i}(t) = A_{\text{eff},\,i} e^{-\left(k_{\text{Tr},i} + k_{\text{ns},i}\right) t} + f_o, \tag{2b}$$

where the index $i = 0$ for the no-force experiments and $i = \text{F}$ for experiments under 9 pN of force. f_{o} represents the fraction of beads that do not detach and can vary between each experimental data set. Equation 2*b* arises directly from the following first-order decay model:

$$\frac{d[\text{beads}]}{dt} = -k_{\text{Tr}}[\text{beads}] - k_{\text{ns}}[\text{beads}]. \tag{3}$$

Rate constants resulting from this analysis are reported in Table 2.

Our data show a substantial increase in the trypsin-dependent cleavage rate as the force increased from 0 to 9 pN: from $k_{\text{Tr},0} = 0.009 \pm 0.013$ min^{-1} to $k_{\text{Tr,F}} = 0.222 \pm 0.018$ min^{-1}. These values were determined by fitting the mean fraction of beads remaining as a function of time (determined from multiple experimental replicates), weighted by the standard error of the mean fraction at each point. Alternative approaches to the data analysis similarly found a significant increase in the rate of collagen cleavage by trypsin (Tables S2 and S3), with rates enhanced 10- to 20-fold at 9 pN of force compared to the no-load condition. This result suggests that as collagen is stretched, the triple helix becomes more susceptible to cleavage by trypsin.

To confirm that the effect of force is on cleavage of collagen rather than of other proteins in the system used as linkers, control experiments were performed. Both streptavidin and BSA, used in the linking chemistry to connect collagen to the surface, have multiple trypsin recognition sites. Thus, the force-enhanced cleavage rate could arise from force-induced destabilization of streptavidin and/or BSA rather than of collagen. To investigate this possibility, we repeated the above experiments but used DNA as a tether in place of collagen. DNA is not a substrate for trypsin; therefore, any trypsin-dependent cleavage observed would arise from cleavage of the linking proteins. These experiments showed no force enhancement of the trypsin-dependent cleavage rate, k_{Tr} (Fig. S4). This result implies that the linking streptavidin and BSA are not destabilized by force exerted through the molecular tether. Thus, these findings indicate that the enhancement of proteolysis is due to a destabilization of collagen's triple helix when stretched, which increases the accessibility of otherwise sterically hindered chains to the protease active site.

The destabilization of collagen's triple helix by force can be compared with previous findings (Table 1). It is possible that shear-induced helix rupture (10) contributes to our force-enhanced bead detachment in the absence of trypsin. However, the loss of tethered beads from the surface, even in the absence of enzyme, does not occur with different surface chemistry (Fig. S6) and so is more likely attributed to mechanically weak linking interactions, perhaps between biotinylated BSA and silane (18).

Force-enhanced cleavage is consistent with conclusions from single-molecule collagen studies that used the collagenase matrix-metalloprotease-1 (MMP1) (9,15), but contradictory to those from studies that used bacterial collagenase (14). Because these enzymes target different sequences of collagen, it is possible that collagen exhibits a sequence-dependent response to applied load. Interestingly, of the 81 possible trypsin sites per type III collagen chain, previous analysis of collagen fragments produced by trypsin proteolysis identified one primary cleavage site (25) located in a "loose" region of the triple helix that is shared by the unique recognition sequence of MMPs (26). The force enhancement of collagen proteolysis by trypsin, as by MMP1, may be a result of both enzymes probing the same region of the collagen triple helix. Indeed, our finding of a non-zero cleavage rate at zero force is consistent with the expectation that type III collagen is weakly susceptible to trypsin digestion in this MMP region in solution at room temperature (25). In contrast to MMP1, trypsin has not evolved to interact with triple-helical collagen and thus may be considered a more passive probe of externally induced changes in collagen's structure.

Just as distinct sequences of triple helix can possess different thermal stabilities and helical pitch (5), it is possible that collagen has a molecular structure whose response to applied force is modulated by its local sequence.

Future experiments could examine this question by using different collagen substrates, such as type I collagen that lacks a trypsin site in the MMP target region, or by using different proteases to target distinct regions of collagen's sequence, thereby mapping the sequence-dependent mechanical stability within the native, full-length protein. How distinct mechanical signatures along the length of each collagen interact with and modulate biochemical and cell biological interactions is an exciting question to pose for future studies. More generally, the real-time, highly multiplexed approach of MR.CFM enables the discovery and characterization of transiently accessible and mechanically cryptic sites within native states of proteins (27), protein-DNA structures, and protein assemblies.

Data availability

The data sets generated and analyzed during the current study are available from the corresponding author on request.

SUPPORTING MATERIAL

Supporting Materials and Methods, six figures, four tables, one movie, and two data files are available at http://www.biophysj.org/biophysj/supplemental/S0006-3495(17)35085-3.

AUTHOR CONTRIBUTIONS

M.W.H.K. and N.R.F. designed the research. M.W.H.K. built MR.CFM and performed all experiments. M.W.H.K. and N.R.F. analyzed the results and wrote the manuscript.

ACKNOWLEDGMENTS

We are grateful to Rachel Altman for insightful discussions regarding data analysis, Aaron Lyons for AFM imaging and analysis, Wesley Wong and Ken Halvorsen for helpful discussions, and David Lee for the use of the bright-field microscope. We thank John Bechhoefer, Edgar Young, and members of the Forde laboratory for critical readings of the manuscript.

This research was funded by a Discovery Grant from the Natural Sciences and Engineering Research Council of Canada (NSERC). M.W.H.K. acknowledges support from Robert Russell Family/First Nations Graduate Awards.

SUPPORTING CITATIONS

Reference (28) appears in the Supporting Material.

REFERENCES

1. Bruckner, P., and D. J. Prockop. 1981. Proteolytic enzymes as probes for the triple-helical conformation of procollagen. *Anal. Biochem.* 110:360–368.
2. Polach, K. J., and J. Widom. 1999. Restriction enzymes as probes of nucleosome stability and dynamics. *Methods Enzymol.* 304:278–298.
3. Park, C., and S. Marqusee. 2004. Probing the high energy states in proteins by proteolysis. *J. Mol. Biol.* 343:1467–1476.
4. Mortimer, G. M., and R. F. Minchin. 2016. Cryptic epitopes and functional diversity in extracellular proteins. *Int. J. Biochem. Cell Biol.* 81:112–120.
5. Shoulders, M. D., and R. T. Raines. 2009. Collagen structure and stability. *Annu. Rev. Biochem.* 78:929–958.
6. Chang, S. W., and M. J. Buehler. 2014. Molecular biomechanics of collagen molecules. *Mater. Today.* 17:70–76.
7. Tonge, T. K., J. W. Ruberti, and T. D. Nguyen. 2015. Micromechanical modeling study of mechanical inhibition of enzymatic degradation of collagen tissues. *Biophys. J.* 109:2689–2700.
8. Chung, L., D. Dinakarpandian, …, H. Nagase. 2004. Collagenase unwinds triple-helical collagen prior to peptide bond hydrolysis. *EMBO J.* 23:3020–3030.
9. Adhikari, A. S., J. Chai, and A. R. Dunn. 2011. Mechanical load induces a 100-fold increase in the rate of collagen proteolysis by MMP-1. *J. Am. Chem. Soc.* 133:1686–1689.
10. Zitnay, J. L., Y. Li, …, J. A. Weiss. 2017. Molecular level detection and localization of mechanical damage in collagen enabled by collagen hybridizing peptides. *Nat. Commun.* 8:14913.
11. Varma, S., M. Botlani, …, J. D. Schieber. 2015. Effect of intrinsic and extrinsic factors on the simulated D-band length of type I collagen. *Proteins.* 83:1800–1812.
12. Sun, Y. L., Z. P. Luo, …, K. N. An. 2002. Direct quantification of the flexibility of type I collagen monomer. *Biochem. Biophys. Res. Commun.* 295:382–386.
13. Wieczorek, A., N. Rezaei, …, N. R. Forde. 2015. Development and characterization of a eukaryotic expression system for human type II procollagen. *BMC Biotechnol.* 15:112.
14. Camp, R. J., M. Liles, …, J. W. Ruberti. 2011. Molecular mechanochemistry: low force switch slows enzymatic cleavage of human type I collagen monomer. *J. Am. Chem. Soc.* 133:4073–4078.
15. Adhikari, A. S., E. Glassey, and A. R. Dunn. 2012. Conformational dynamics accompanying the proteolytic degradation of trimeric collagen I by collagenases. *J. Am. Chem. Soc.* 134:13259–13265.
16. Eckhard, U., E. Schönauer, …, H. Brandstetter. 2011. Structure of collagenase G reveals a chew-and-digest mechanism of bacterial collagenolysis. *Nat. Struct. Mol. Biol.* 18:1109–1114.
17. Sbalzarini, I. F., and P. Koumoutsakos. 2005. Feature point tracking and trajectory analysis for video imaging in cell biology. *J. Struct. Biol.* 151:182–195.
18. Hua, B., K. Y. Han, …, T. Ha. 2014. An improved surface passivation method for single-molecule studies. *Nat. Methods.* 11:1233–1236.
19. Shayegan, M., N. Rezaei, …, N. R. Forde. 2013. Probing multiscale mechanics of collagen with optical tweezers. *In* Proceedings of the SPIE. K. Dholakia and G. C. Spalding, eds. SPIE, pp. 88101–88110.
20. Gasteiger, E., C. Hoogland, …, A. Bairoch. 2005. Protein Identification and Analysis Tools on the ExPASy Server. *In* The Proteomics Protocols Handbook. J. M. Walker, ed. Humana Press, pp. 571–607.
21. Halvorsen, K., and W. P. Wong. 2010. Massively parallel single-molecule manipulation using centrifugal force. *Biophys. J.* 98:L53–L55.
22. Neuman, K. C., and A. Nagy. 2008. Single-molecule force spectroscopy: optical tweezers, magnetic tweezers and atomic force microscopy. *Nat. Methods.* 5:491–505.
23. Hoang, T., D. S. Patel, and K. Halvorsen. 2016. A wireless centrifuge force microscope (CFM) enables multiplexed single-molecule experiments in a commercial centrifuge. *Rev. Sci. Instrum.* 87:083705.
24. Yang, D., A. Ward, …, W. P. Wong. 2016. Multiplexed single-molecule force spectroscopy using a centrifuge. *Nat. Commun.* 7:11026.

25. Miller, E. J., J. E. Finch, Jr., …, P. B. Robertson. 1976. Specific cleavage of the native type III collagen molecule with trypsin. Similarity of the cleavage products to collagenase-produced fragments and primary structure at the cleavage site. *Arch. Biochem. Biophys.* 173:631–637.

26. Fields, G. B. 1991. A model for interstitial collagen catabolism by mammalian collagenases. *J. Theor. Biol.* 153:585–602.

27. Gordon, W. R., B. Zimmerman, …, S. C. Blacklow. 2015. Mechanical allostery: evidence for a force requirement in the proteolytic activation of Notch. *Dev. Cell.* 33:729–736.

28. Shayegan, M., T. Altindal, …, N. R. Forde. 2016. Intact telopeptides enhance interactions between collagens. *Biophys. J.* 111: 2404–2416.

Biophysical Journal, Volume *114*

Supplemental Information

Single-Molecule Assay for Proteolytic Susceptibility: Force-Induced Collagen Destabilization

Michael W.H. Kirkness and Nancy R. Forde

Supporting Note 1: Mini-Radio Centrifuge Force Microscope (MR.CFM) Design and Use

Centrifuge

MR.CFM fits within a single bucket of a Beckman Coulter Allegra X-12R centrifuge, equipped with an SX4750A ARIES "Swinging Bucket" Rotor Assembly. The centrifuge is refrigerated, enabling easy access to temperature-controlled single-molecule force assays. Design constraints from this bucket assembly are its rotational arm length of 207.8 mm, a maximal rotational speed of 3750 RPM, and a maximum fluid mass per bucket of 750 g, with an imbalance tolerance of ±50 g.

MR.CFM Microscope

The use of a benchtop centrifuge prescribed three design limitations: overall height (180 mm) and mass (750 g) (set by the specific centrifuge and rotor), and the need for wireless communication and power. The final microscope accommodates all of these constraints, with a height of 154 mm, a mass of 421 g (including batteries), and fully wireless operation. MR.CFM is depicted in Figure 2 of the main manuscript. The instrument was built using as many commercial parts as possible for ease of reproduction. Schematics and parts lists are provided in Supporting Figure 1 and Supporting Table 1. Note that, while the designs provided are specific to this rotor assembly, MR.CFM can easily be adapted for other benchtop centrifuges, primarily by modifying the base.

MR.CFM is composed of two parts, the optical assembly and the base, which provides support and acts as a sample holder. A hard, closed-cell plastic (Sintra) formed the bulk of the base, chosen for its high rigidity and low mass. An aluminum insert was included directly below the microscope within this base to strengthen the rigidity of the assembly under high load and provide support for the sample chamber. These parts were machined to fit snugly into the centrifuge bucket (Supporting Figure 2 and Supporting CAD drawings).

The optical path comprises an LED light source, ground glass diffuser, sample chamber, infinity-corrected objective lens, tube lens, and CCD camera with lens (Supporting Figure 1c and Supporting Table 1). The LED light source and ground glass diffuser are housed within the aluminum insert while the sample chamber slides into the sample holder on top of the aluminum insert (Supporting Figure 2). The LED and sample chamber are held in place simply by friction, which facilitates their replacement, while the diffuser is glued (JB Weld Original) into the insert. The remaining components in the optical path are mounted within stacking lens tubes. The following non-standard-sized parts are glued into place using epoxy (JB Weld Original): aluminum base insert, inner portion of the objective lens CCD camera with lens and extension mount (see below). The tube lens is held in place using a counter-threaded locking ring. The microscope's focal distance is modified by manually rotating two adjustable lens tubes, thereby altering the distance between the objective and tube lens. The focus is locked in place by tightening a counter-threaded locking ring. Two parts were removed from the objective lens: a rubber spacer from the lens stack (which resulted in a significantly enhanced stability of the working distance under force) and the outer casing (which reduced the mass by 67 g).

Pixel size in the microscope field of view was determined to be 0.43 μm/px, using a transmission electron microscopy grid (Ted Pella) and analysis using ImageJ.

Supporting Note 2: Image Acquisition and Analysis

The image analysis workflow acquires, processes and analyzes data from the raw images acquired by MR.CFM (Figure 3). The camera produces a wireless analog signal, which is received by the radio AV receiver. The transfer rate is 28 frames per second. In this step, there is some inherent interference that is coupled to the rotation frequency of the rotor with MR.CFM. Experimentally, this interference can be minimized by placing the AV receiver directly above the rotor's spindle. A USB analog-to-digital converter converts the analog signal from the AV receiver to digital. The signal is then acquired by a computer program, Totalmedia 3.5 (ArcSoft), which permits storage and viewing of the image stream in real-time. Real-time transfer of the data to an external computer is beneficial as it allows for essentially unlimited storage, permitting extremely long run times. In our instrument, run lengths are hardware-limited by battery lifetimes: three hours of continuous measurement are possible with two 9 V batteries wired in parallel to power the camera; this is easily increased by the addition of more batteries in parallel.

Efficient analysis requires the ability to count hundreds to thousands of particles reliably. The image processing used in this work minimizes user input and is implemented within a semi-automated ImageJ macro (code provided online). First, to remove any interference remaining in the signal (arising from rotation of the microscope about the receiver), a 10-image median z-stack algorithm is first applied, which eliminates the interference. Next, a rolling ball subtraction method (50 pixels) is applied, which improves image quality by subtracting the image background. The script then inverts the images and sums five images to increase contrast. Before counting, we mask regions corresponding to uncountable regions (such as multiple particle

clusters and dust). In cases where the contrast is not sufficient, a local adaptive thresholding plugin is used prior to particle counting, which removes the background completely.

Supporting Note 3: Proteolysis of Collagen and DNA by Trypsin

Surface Chemistry

For highly multiplexed experiments in the MR.CFM, it is essential to have a high surface coverage of beads, each bound to the surface by a single collagen molecule. Here, we implemented a blocking and specific tethering system that relies on a self-assembled monolayer (SAM) of Tween-20 for blocking and on biotinylated BSA for specific tethering.[1] To form the SAM, glass slides and coverslips were cleaned and activated through a series of washes with potassium hydroxide and organic solvents, followed by a coating of dichlorodimethylsilane (DDS). DDS (Sigma 440272) creates a strongly hydrophobic surface on the glass slide. Self-assembly of the Tween-20 surfactant resulted in a densely coated short PEG layer to block nonspecific binding of both the microspheres and enzymes (Figure 2d). To enable specific binding, biotinylated BSA was applied before Tween-20, and was bound by streptavidin.

The detailed protocol followed Hua *et al*.,[1] with the following minor modifications. As stated above, glass coverslips and slides were used, and a glass dish was used for coating rather than a glass slide holder. Thus, we used 200 ml of hexane and 133 µl DDS. Assembly of our chambers used JB Weld instead of double-sided tape. For the surface coating, we incubated for 10 minutes with 0.5 mg/ml biotinylated BSA (Sigma A8549) in 20 mM Tris and 50 mM NaCl, pH 8.0; followed by 10 minutes with 0.2% Tween-20 (Sigma P9416); followed by a 5-minute incubation with 0.5 mg/ml streptavidin (Sigma S4762) in 20 mM Tris and 50 mM NaCl, pH 8.0. Final washing steps were performed using our reaction buffer of 100 mM Tris, 400mM NaCl, pH 7.4.

Collagen Functionalization and Tethering

Recombinant human type III collagen (Fibrogen FG-5016) was end-labelled for manipulation as described.[2] Briefly, its N-terminus was labeled with a biotin via aldehyde functionalization (PLP, Sigma P9255) and further reaction with biotin hydrazide (Sigma B7639) to form a covalent hydrazone bond with the introduced aldehyde. The success of the reaction was confirmed with Western blots using streptavidin alkaline phosphatase. Biotinylated collagen was tethered to the bead via its unique C-terminal cysteine residues. Amine-functionalized superparamagnetic microspheres (M270 Dynabeads) were modified by reaction with an SPDP linker (Pierce 21857). Concurrently, collagen was reduced with TCEP reducing gel (Thermo Scientific 77712) to present thiols. Incubation of reduced collagen with SDPD-functionalized beads allowed for the formation of disulfide bonds between beads and collagen proteins. The ratio of collagen:beads for this reaction was adjusted to achieve single-molecule tethers, as follows.

As the ratio of collagen:beads was decreased in this final coupling step, we observed that the number of beads bound to the surface decreased. This implied that collagen concentration was the limiting factor for forming tethers, suggesting we were in the single-tether range. To confirm that single tethers were linking the beads to the surface, we visually inspected the beads at high magnification to confirm constrained, two-dimensional Brownian motion.

DNA Preparation

To use the same surface conjugation methods as for collagen, DNA end-labelled with thiol and aldehyde reactive groups was produced via PCR from the pUC19 plasmid. The PCR product was 969 bp, approximately the same contour length as collagen (~300 nm). The PCR used a thiol-

modified primer, 5'-Thiol TTG CTT GAT ATC TTG TAC TGA GAG TGC ACC-3', and an aldehyde-modified primer, 5'- Aldehyde TGT CTT AGA TCT TTT GGA GCG AAC GAC-3' (both from Bio-Synthesis). DNA was tethered to the amine-functionalized microspheres (M270 Dynabeads) via the same reaction pathway as collagen.

Single-Molecule Proteolysis Experiments

Immediately prior to measurements, trypsin and labelled (DNA or collagen) beads were mixed and injected into the sample chamber. The sample chamber was sealed with melted paraffin wax and placed upside down for approximately five minutes to allow the labelled beads to settle and bind to the desired surface. The chamber was then inverted and inserted into MR.CFM, its focus was adjusted, and the entire MR.CFM was placed in the centrifuge. When the centrifuge reached the desired rotation rate (for these experiments, 800 rpm), image recording (Totalmedia 3.5) was initiated on the remote computer. Parallel experiments with collagen (or DNA) under ~zero force (67 fN, the force of gravity on the beads) were conducted essentially as above, but with imaging performed using a bright-field microscope (Olympus BX51, equipped with 10X Plan N objective) and CCD camera (Flea, Point Grey Research), and with images acquired using National Instruments LabVIEW.

The force acting on the beads in MR.CFM was calculated from $F=m\omega^2 r$, where the rotational arm length r=18.2 cm from the centre of the spindle to the sample chamber, and the mass of the beads relative to water m=6.9x10^{-12} g is obtained from the manufacturer-specified bead density (1.6 g/cm^3) and size (2.8 μm diameter), which has been validated previously in single-molecule force measurements.[3]

Experimental Replicates and Error Determination

Multiple replicates were performed as follows. Trypsin force experiments include data from six separate runs, on four different days, with a total number of initial particles of N=4903. Trypsin zero-force experiments include data from four separate runs, on four different days, with N=12131. No enzyme, force experiments use data from three separate runs, on three different days, with N=1493. No enzyme, zero-force experiments use data from two separate runs, on two different days, with N=4252. Complete data sets are shown in Supporting Figure 5.

Supporting Table 1 – MR.CFM parts list

Component	**Description, source, part number and price (USD)**
Base	Sintra plastic, machined as in Supporting Figure 2. Approximate cost for starting material: $20 (Associated Plastics).
Base insert	Aluminum, machined as in Supporting Figure 2. Approximate cost for starting material: $3 (Metal Supermarkets).
LED with holder	5W white. Super Bright LEDs Inc. VL-H01xWx5 ($7)
Ground Glass Diffuser	Thor Labs DG05-120 ($13)
Infinity-corrected objective lens	40X, NA 0.65, air. Nikon (<$500)
Lens tubes with internal and external locking rings	2x Stackable; 1” diameter. ThorLabs SM1L10 ($15) 3x Adjustable; 1” diameter. ThorLabs SM1V10 ($35)
Tube lens	40 mm focal length. Thor Labs LA1422 ($22)
Camera lens	Included with camera.
Camera lens extension mount	Aluminum, machined to provide desired magnification (Supporting Figure 2). Approximate cost for starting material: $1 (Metal Supermarkets).
Wireless CCD Camera	Security Color Mini Spy Pinhole CCD Wireless Camera. RC Hobbies Outlet 73724810. Alternatively, HDE Pinhole Mini Wireless Camera, Amazon ($25)
Lithium 3V “coin” batteries	2x2032; widely available ($1)
9V Batteries + snap connector clips	Widely available ($1)
Radio AV Receiver	Included with wireless camera
TV Tuner	AVI TV Wonder HD 750 USB. Alternatively, StarTech S-Video / Composite to USB Video Capture Cable, B&H ($35)

Supporting Table 2 – Rate constants from combined replicates

Experiment	k_{eff} (min^{-1})	k_{ns} (min^{-1})	k_{Tr} (min^{-1})
-trypsin, F=0	--	0.010 ± 0.013	--
+trypsin, F=0	0.018 ± 0.001	0.010* ± 0.013	0.007 ± 0.013
-trypsin, F=9 pN	--	0.137 ± 0.005	--
+trypsin, F=9 pN	0.364 ± 0.037	0.137* ± 0.005	0.227 ± 0.037

Rate constants were determined by weighting $f(t)$ determined from the total number of beads remaining at each time ($f(t) = N_{tot}(t)/N_{tot}(0)$) by the counting error ($1/\sqrt{N}$).

*Values from the no-enzyme fits were used to determine the trypsin-dependent rate constants, using equations (1) and (2).

Supporting Table 3 – Rate constants from individual collagen replicates

Experiment	Replicate number	Initial number of beads	k_{eff} (min^{-1})	$<k_{eff}>$ (min^{-1})	$<k_{ns}>$ (min^{-1})	$<k_{Tr}>$ (min^{-1})
-trypsin, F=0	1	1929	0.009 ± 0.015	--	0.011 ± 0.002	--
	2	2323	0.012 ± 0.019			
+trypsin, F=0	1	3461	0.050 ± 0.008	0.039 ± 0.020	0.011* ± 0.002	0.028 ± 0.021
	2	2918	0.054 ± 0.010			
	3	3384	0.009 ± 0.001			
	4	2368	0.044 ± 0.006			
-trypsin, F=9 pN	1	775	0.163 ± 0.010	--	0.160 ± 0.003	--
	2	182	0.157 ± 0.022			--
	3	536	0.160 ± 0.020			
+trypsin, F=9 pN	1	935	0.210 ± 0.008	0.362 ± 0.188	0.160* ± 0.003	0.202 ± 0.188
	2	860	0.360 ± 0.011			
	3	501	0.188 ± 0.010			
	4	743	0.281 ± 0.010			
	5	1187	0.436 ± 0.006			
	6	677	0.697 ± 0.032			

Errors on the individual k_{eff} represent 1σ on the fit parameters. The error on each mean rate constant represents the standard deviation of the individual k_{eff} values.

Replicates with force were fit to 20 minutes. Replicates without force were fit to 60 minutes, with the exception of replicate 3 with trypsin, which was fit to 180 minutes to permit fit convergence.

*Values from the no-enzyme fits were used to determine the trypsin-dependent rate constants, using equations (1) and (2).

Supporting Table 4 – Rate constants from individual DNA replicates

Experiment	Replicate number	Initial number of beads	k_{eff} (min^{-1})	$<k_{eff}>$ (min^{-1})	$<k_{ns}>$ (min^{-1})	$<k_{Tr}>$ (min^{-1})
-trypsin, F=0	1	622	0.006 ± 163	--	0.026 ± 0.012	--
	2	833	0.041 ± 0.27			
+trypsin, F=0	1	250	0.205 ± 0.277	0.140 ± 0.092	0.026* ± 0.012	0.114 ± 0.092
	2	1029	0.124 ± 0.049			
-trypsin, F=9 pN	1	18	0.138 ± 0.055	--	0.233 ± 0.032	--
	2	168	0.270 ± 0.018			
	3	83	0.256 ± 0.015			
	4	252	0.248 ± 0.039			
	5	369	0.206 ± 0.028			
+trypsin, F=9 pN	1	150	0.120 ± 0.015	0.217 ± 0.08	0.233* ± 0.032	~0
	2	41	0.180 ± 0.035			
	3	242	0.200 ± 0.008			
	4	220	0.232 ± 0.010			
	5	113	0.366 ± 0.023			

Errors on the individual k_{eff} represent 1σ on the fit parameters. The error on each mean rate constant represents the standard deviation of the individual k_{eff} values.

*Values from the no-enzyme fits were used to determine the trypsin-dependent rate constants, using equations (1) and (2).

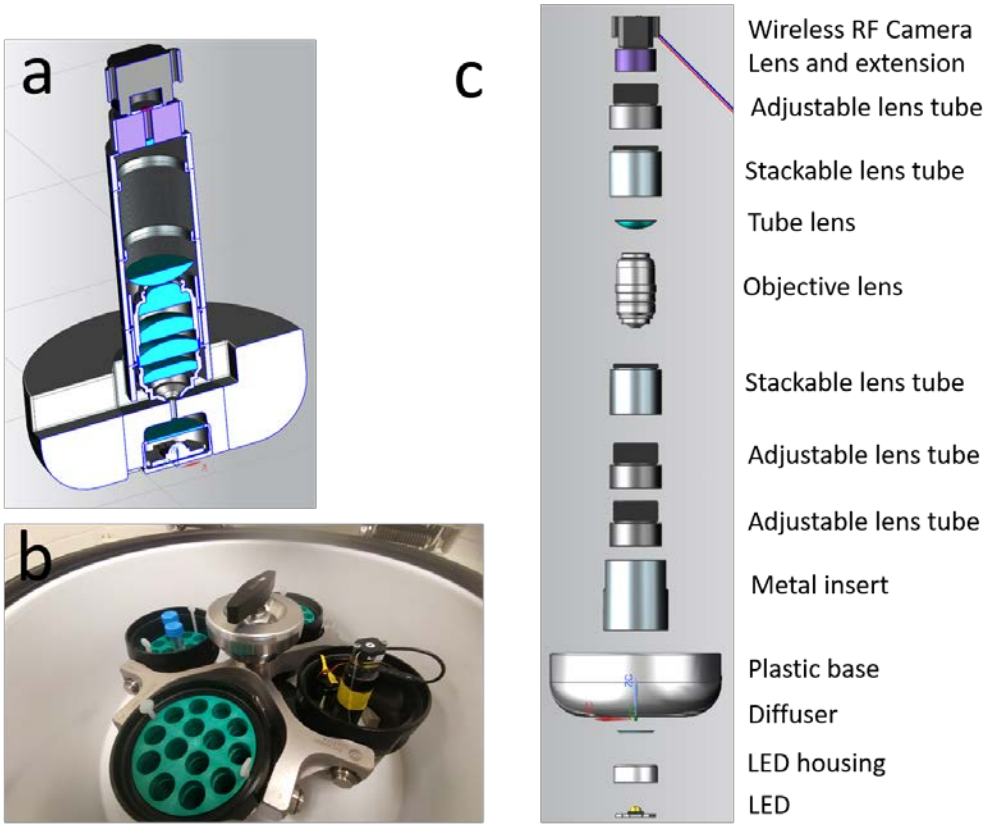

Supporting Figure 1. MR.CFM model and assembly. a) To-scale 3D rendering of MR.CFM. MR.CFM fits inside a centrifuge bucket and has a total height of 154 mm and mass 421 g, including batteries. b) MR.CFM is shown inside a centrifuge bucket within a Beckman Coulter Allegra X-12R centrifuge (SX4750A ARIES™ Rotor Swinging Bucket). c) Assembly of parts of MR.CFM.

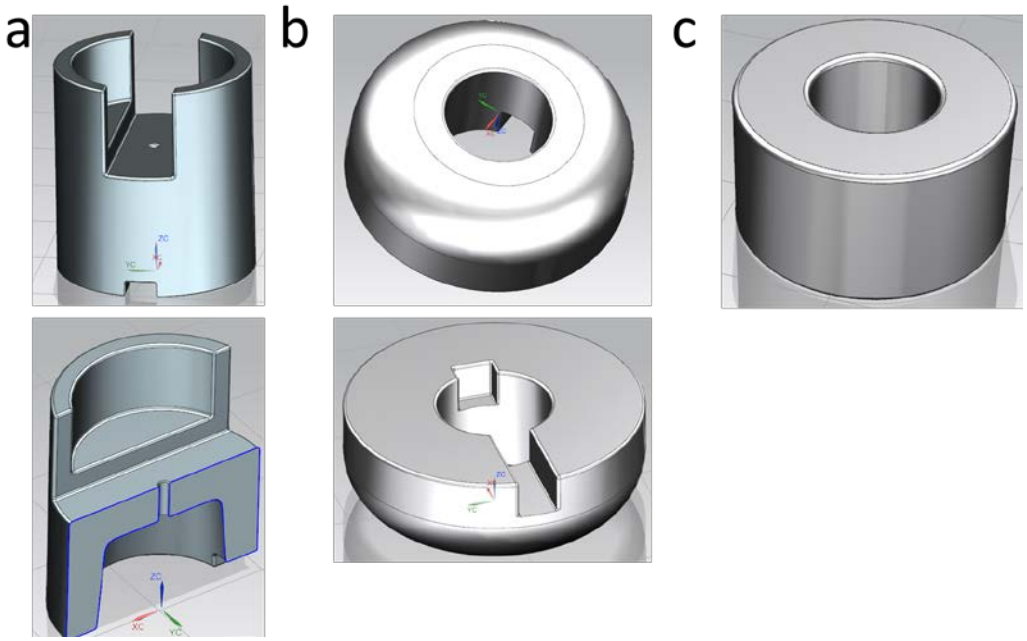

Supporting Figure 2. Drawings of the custom-made parts. (a) Sintra plastic base. (b) Aluminum base insert with sample chamber slot. (c) Pinhole lens extension mount. CAD drawings are available as Supporting Files online.

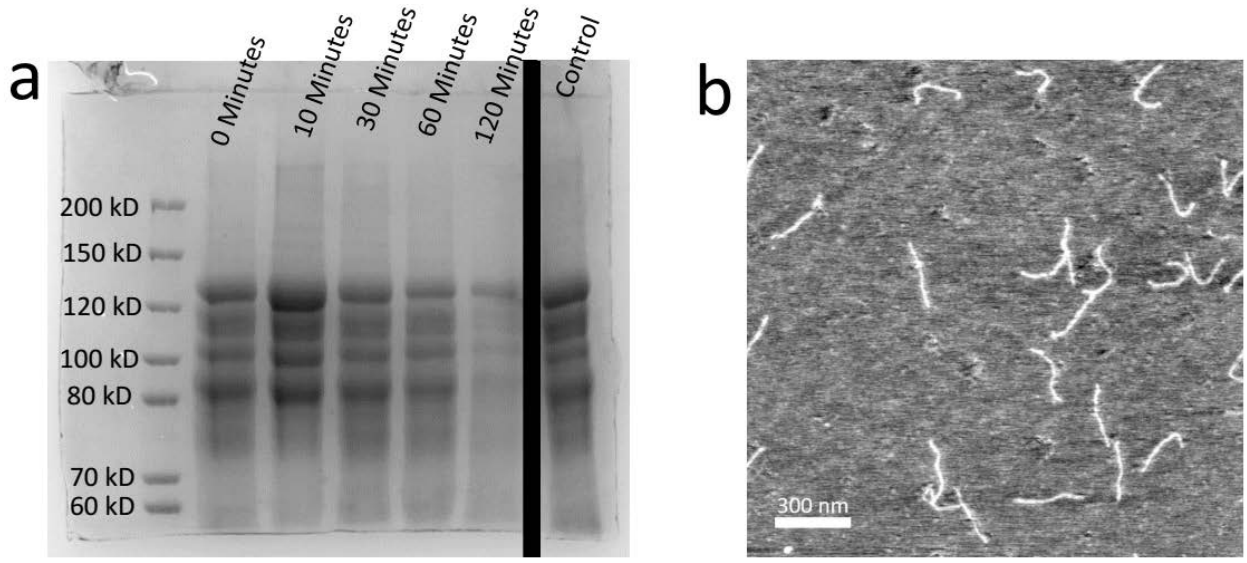

Supporting Figure 3. Time-dependent trypsin cleavage of type III collagen and AFM characterization. (a) Trypsin can cleave collagen at room temperature without force, as noted by the gradual disappearance of defined bands in the gel. The conditions for the reaction are 2 mg/ml type III collagen and 1 μg/ml trypsin (a much lower concentration than used in the single-molecule assays), in a buffer of 0.1M Tris, 0.4M NaCl at a pH of 7.4. Aliquots were removed at 0, 10, 30, 60 and 120 minutes respectively, then heated for 10 minutes at 90°C in the presence of β-mercaptoethanol. The samples were run on a 6% SDS-PAGE gel and stained with a solution of Coomassie blue. Of note, SDS-PAGE gels of pure collagen can exhibit shorter bands (as seen here, running at approximately 115, 100, and 80 kDa), which likely arise from acid-induced hydrolysis at 90°C.[4] The stock solution is monodisperse, as seen in (b), AFM image of type III collagen molecules. Analysis of contour lengths from this and other images gives 269 +/- 2 nm (*N*=33), demonstrating that the collagen sample is monodisperse. Collagen was deposited from 1 mM HCl, 100 mM KCl onto mica and then dried prior to imaging. Images were recorded with an Asylum Research MFP-3D SPM in tapping mode, with Mikromasch HQ:NSC15/AL BS tips.

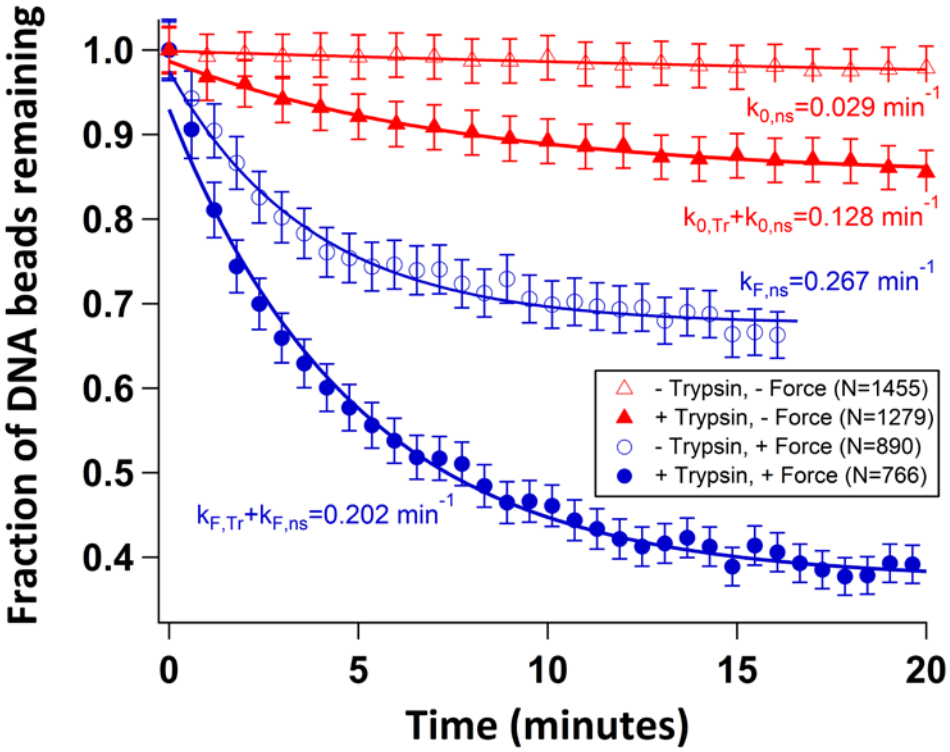

Supporting Figure 4. DNA molecules tethered using the same linking chemistry do not exhibit a force-enhanced cleavage rate by trypsin. This demonstrates that the streptavidin and BSA linking proteins are not responsible for the force-induced susceptibility to proteolysis. Here, the data from all replicates are pooled to provide the overall fraction of beads remaining as a function of time. Error bars represent $\sqrt{N(t)}$ counting errors. The fraction of beads remaining as a function of time is well described by a single exponential decay. The effective rate constants resulting from fitting these data are shown in the figure. Rate constants from single exponential fits to each replicate are reported in Supporting Table 4 and do not differ significantly from the values shown here. Both approaches find that the trypsin-dependent cleavage rate k_{Tr} is not enhanced by force.

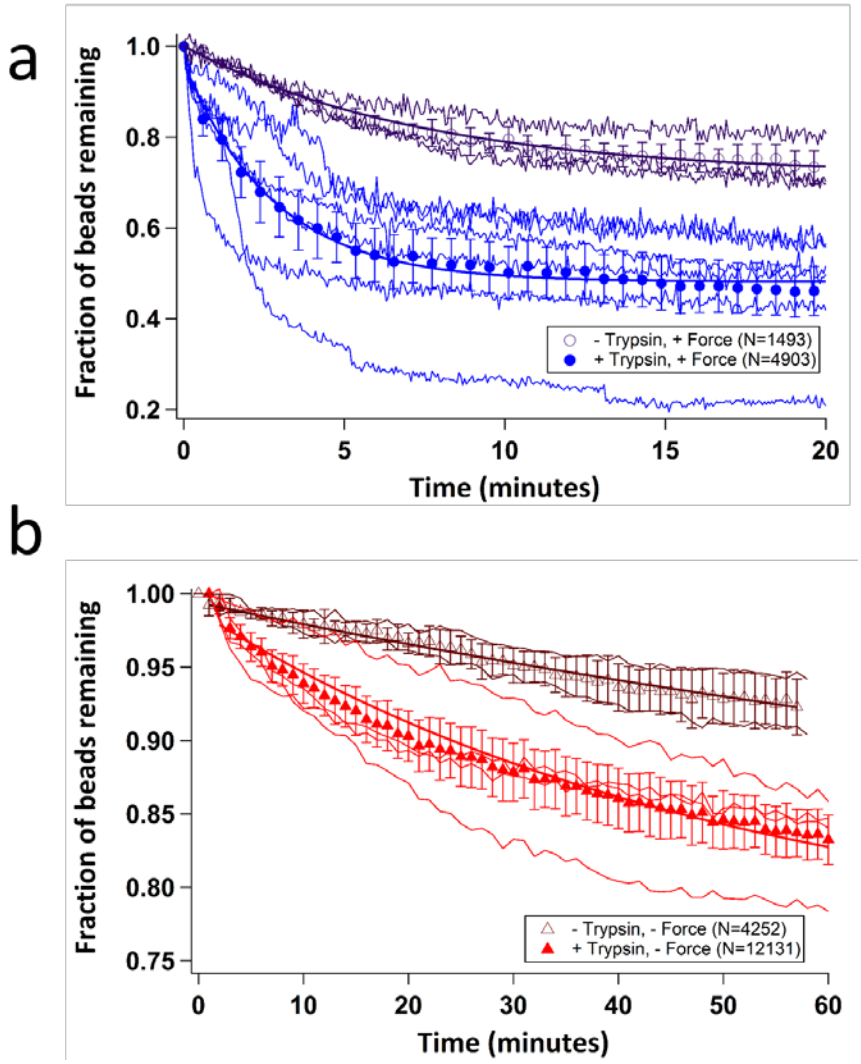

Supporting Figure 5. Full data sets for single-molecule collagen experiments, shown separately as (a) with force and (b) without force. Individual replicates are shown as thin lines (with variation due to imperfect counting of very large numbers of beads), and the average fraction remaining is shown in symbols, corresponding to Figure 4a in the main text.

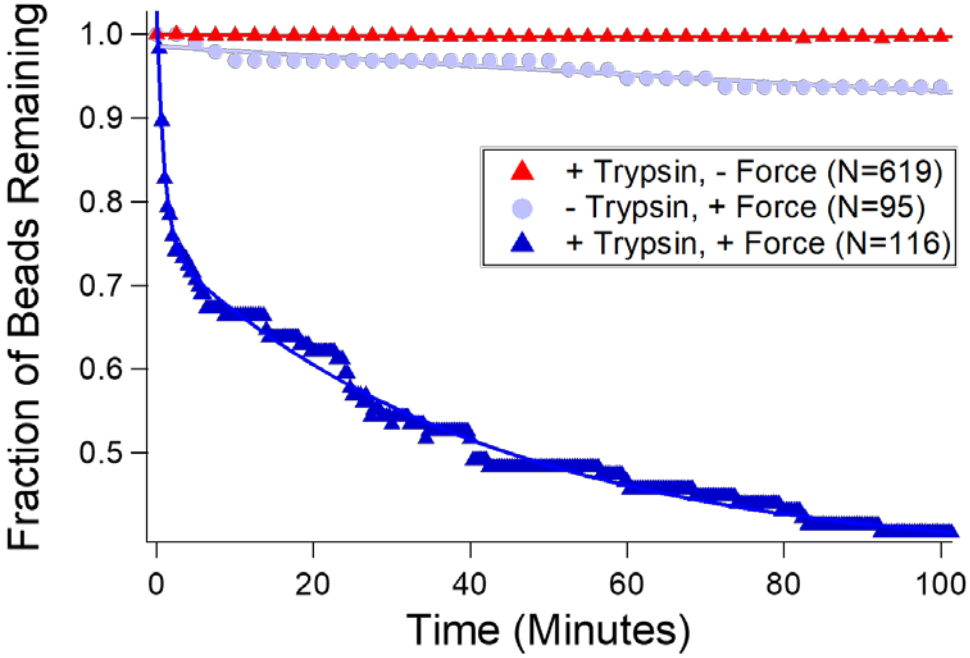

Supporting Figure 6. Force-enhanced collagen cleavage by trypsin is observed also in chambers with a different surface treatment. Here, surfaces were blocked with BSA only. Very little force-induced detachment of collagen beads was observed, in contrast to the DDS- and Tween-coated surfaces (Figure 4 and Supporting Figure 5). The trypsin cleavage curve is well described by a double exponential decay; this may arise from the loss of trypsin from solution to the surface and/or contributions from beads tethered to the surface by more than one collagen. Many fewer tethered particles were observed with this surface treatment.

Supporting References

1. Hua, B. et al. An improved surface passivation method for single-molecule studies. *Nat Meth* **11**, 1233-1236 (2014).
2. Shayegan, M. et al. in Proceedings of the SPIE, Vol. 8810. (eds. K. Dholakia & G.C. Spalding) 88101P (SPIE, San Diego; 2013).
3. Yang, D., Ward, A., Halvorsen, K. & Wong, W.P. Multiplexed single-molecule force spectroscopy using a centrifuge. *Nat Commun* **7**, 11026 (2016).
4. Shayegan, M., Altindal, T., Kiefl, E. & Forde, N.R. Intact Telopeptides Enhance Interactions between Collagens. *Biophys J* **111**, 2404-2416 (2016).